AIAA JOURNAL
Vol. 31, No. 4, April 1993

Coupling Between a Supersonic Boundary Layer and a Flexible Surface

Abdelkader Frendi*
Analytical Services and Materials, Inc., Hampton, Virginia 23665
Lucio Maestrello†
NASA Langley Research Center, Hampton, Virginia 23665
and
Alvin Bayliss‡
Northwestern University, Chicago, Illinois 60035

The coupling between a two-dimensional, supersonic, laminar boundary layer and a flexible surface is studied using direct numerical computations of the Navier-Stokes equations coupled with the plate equation. The flexible surface is forced to vibrate by plane acoustic waves at normal incidence emanated by a sound source located on the side of the flexible surface opposite to the boundary layer. The effect of the source excitation frequency on the surface vibration and boundary-layer stability is analyzed. We find that, for frequencies near the fifth natural frequency of the surface or lower, large disturbances are introduced in the boundary layer that may alter its stability characteristics. The interaction between a stable two-dimensional disturbance of Tollmien-Schlichting (TS) type with the vibrating surface is also studied. We find that the disturbance level is higher over the vibrating flexible surface than that obtained when the surface is rigid, which indicates a strong coupling between flow and structure. However, in the absence of the sound source, the disturbance levels over the rigid and flexible surfaces are identical. This result is due to the high frequency of the TS disturbance that does not couple with the flexible surface.

Introduction

IN recent years, the demand for developing a high-speed civil transport has increased. This has led to an increase in research activity on compressible supersonic flows, in particular on the evolution of unsteady disturbances in a supersonic laminar boundary layer. One class of unsteady disturbances that has received considerable attention is instability waves in a boundary layer, i.e., eigenmodes of the compressible Orr-Sommerfeld equations obtained via linearization around a parallel flow. When these waves are unstable, small disturbances can evolve to large nonlinear disturbances as they propagate downstream in the boundary layer, leading to transition from laminar to turbulent flow.

The linear stability of compressible laminar boundary layers has been studied extensively for both subsonic and supersonic flow regimes. These studies have led to the well-known partition of instabilities into two different classes: the viscosity-dominated class known as the vorticity or first mode, which is similar to the Tollmien-Schlichting (TS) type waves found in low-speed flows, and the acoustic or higher modes.[1-3] At high Mach numbers (>3, for adiabatic conditions), it is found that the dominant modes of instability are the acoustic ones, specifically the first acoustic mode known as the second mode. The linear stability of a two-dimensional flat plate boundary layer including both the vorticity and the acoustic modes has been studied extensively by Mack.[4-6]

Received May 2, 1992; presented as Paper 92-009 at the DGLR/AIAA 14th Aeroacoustics Conference, Aachen, Germany, May 11-15, 1992; revision received Aug. 4, 1992; accepted for publication Aug. 4, 1992.

*Research Scientist. Member AIAA.
†Research Scientist. Associate Fellow AIAA.
‡Professor.

Most of the studies on supersonic boundary-layer stability were performed for flows over rigid surfaces. However, most aircraft structures are made up of flexible surfaces; therefore it is very important to study the interaction (if any) between such structures and unsteady disturbances in the boundary layer. It is known that the unsteady pressure field in the boundary layer can induce significant vibrations of the flexible surface. The vibrating surface can radiate sound over a broad range of frequencies. These acoustic disturbances can 1) excite TS-type waves in the boundary layer and 2) possibly change the stability characteristics so as to enhance the instability of these waves. In turn the TS-type waves can excite vibrations of the flexible surface leading to a positive feedback that may promote an earlier transition. It is therefore important to determine the coupling between unsteady disturbances and a vibrating surface.

In a previous paper[7] we considered the behavior of unstable, second-mode disturbances in a high-speed boundary layer over a flexible surface. It was shown that, although the disturbances were unstable and exhibited substantial growth over the surface, there was little excitation of the flexible surface. This was due to the frequency range of the second-mode disturbances, which were too high to effectively couple with the flexible surface.

In this paper we consider the coupling of a flexible surface with two-dimensional first-mode (i.e., TS-type) disturbances. For the Mach number and Reynolds number considered in this paper, the two-dimensional disturbance exhibits a very small growth near the inflow and then decays with the downstream distance. Even though the disturbance frequency is an order of magnitude lower than that considered previously,[7] we find that the two-dimensional disturbance does not effectively couple with the flexible surface and that there are no significant differences between the evolution of the disturbance over a flexible or rigid surface.

However, a stronger coupling of the flexible surface with the boundary layer can be obtained when the surface is forced by an acoustic disturbance located on the side of the flexible surface opposite to the boundary layer. Acoustic excitation of this sort can lead to large disturbances in the boundary layer. The effectiveness of the flexible surface in transmitting acoustic energy into the boundary layer is highly sensitive to the frequency of the acoustic excitation and the parameters of the flexible surface, in particular the damping. At the present time the computational model is limited to two dimensions and to infinitesimal surface vibrations. However, within these limitations there are indications that the disturbances introduced by the vibrating surface can serve to destabilize the flowfield and that surface vibration should be considered as a potentially destabilizing mechanism that should be accounted for in stability studies.

The remainder of this paper is organized as follows: first the mathematical model is presented, then the numerical scheme used to solve the set of partial differential equations is described, and finally the numerical results and conclusions are presented.

Formulation of the Model

As shown in Fig. (1), three computational domains are being considered: the flow region above the surface, the flexible surface itself, and the no-flow region below the surface. The governing equations in the supersonic flow region are the two-dimensional, compressible, Navier-Stokes equations. In a Cartesian coordinate system, x and y, these equations can be written in conservation form as

$$Q_t = F_x + G_y \tag{1}$$

where Q is the vector $(\rho, \rho u, \rho v, E)^T$, ρ the density, ρu and ρv the x and y momenta, respectively, and E the total energy per unit volume given by

$$E = \tfrac{1}{2}\rho(u^2 + v^2) + \rho c_v T \tag{2}$$

In Eq. (1), the functions F and G are

$$F = \begin{pmatrix} \rho u \\ \rho u^2 + p - \tau_{xx} \\ \rho uv - \tau_{yx} \\ u(E+p) - u\tau_{xx} - v\tau_{yx} - \kappa T_x \end{pmatrix}$$

$$G = \begin{pmatrix} \rho v \\ \rho uv - \tau_{xy} \\ \rho v^2 + p - \tau_{yy} \\ v(E+p) - u\tau_{yx} - v\tau_{yy} - \kappa T_y \end{pmatrix} \tag{3}$$

where τ_{ij} are the components of the viscous stress tensor and κ is the thermal conductivity. In addition to Eq. (1), an ideal gas state equation is used,

$$p = \rho R T \tag{4}$$

where p is the pressure, ρ the density, R the gas constant, and T the temperature. The viscosity is obtained from Sutherland's law

$$\mu = \frac{c_1 T^{3/2}}{T_1 + T} \tag{5}$$

with $T_1 = 198.6°\text{R}$, and $c_1 = 3.66 \times 10^{-7}$ Ns/(m^{2}R$^{1/2}$) for air.

The equation describing the motion of the flexible surface is

$$D\frac{\partial^4 w}{\partial x^4} + \rho_p h \frac{\partial^2 w}{\partial t^2} + \gamma \frac{\partial w}{\partial t} = p^- - p^+ \tag{6}$$

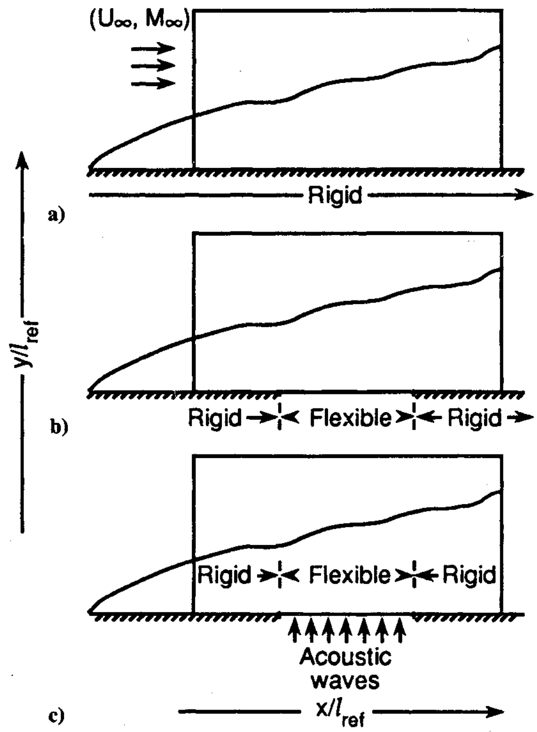

Fig. 1 Computational domains: a) rigid surface, b) flexible surface without sound, c) flexible surface with sound.

where w is the plate transverse deflection, ρ_p the mass per unit volume of the plate, h the plate thickness, and γ the physical damping. In Eq. (6), $D = Mh^3/12(1 - \nu^2)$ is the stiffness of the plate, with M being the modulus of elasticity and ν the Poisson ratio of the plate material. The terms p^+ and p^- are the pressure fields in the flow and no-flow regions, respectively. From the solution of the Navier-Stokes equations we obtain p^+. For p^-, two cases are studied; first when a sound source is used, we consider an imposed pressure field of the form,

$$p^- = p_0^- + \epsilon_1 \sin(\omega_1 t) \tag{7}$$

where ϵ_1 and ω_1 are the amplitude and frequency of the acoustic source, respectively. In the absence of the sound source, an approximation to the solution of the wave equation

$$p^- = p_0^- - (\rho c)_0^- \frac{\partial w}{\partial t} \tag{8}$$

is used. This is similar to the approximation presented by Miksis and Ting.[8] The variables p_0^- and $(\rho c)_0^-$ are the freestream pressure, density, and speed of sound in the region below the surface. A physical situation where Eq. (8) can be used is that of flow over a fuselage surface, and Eq. (7) is a simplification of flow over a vibrating flexible surface excited by engine noise. Since the geometry used is that of a flat surface, the computations were limited to the case of small deflections (order of the plate thickness). The coupling between the boundary layer and the plate is achieved by imposing the vertical velocity of the plate to be one of the boundary conditions for Navier-Stokes equations. Similarly, the surface motion is driven by the pressure field in the boundary layer.

Method of Solution

The unsteady Navier-Stokes equations [Eq. (1)] are solved using an explicit finite difference scheme. The scheme, which is a generalization of MacCormack's scheme obtained by Gottlieb and Turkel,[9] is fourth order accurate on the convective terms, second order accurate on the diffusive terms, and second order accurate in time. The numerical scheme, applied to a one-dimensional equation of the form

$$u_t = F_x \tag{9}$$

consists of a predictor step given by

$$u_i^* = u_i^n + \frac{\Delta t}{6\Delta x}(-7F_i + 8F_{i+1} - F_{i+2}) \tag{10}$$

followed by a corrector step of the form

$$u_i^{n+1} + ½\left[u_i^* + u_i^n + \frac{\Delta t}{6\Delta x}(7F_i^* - 8F_{i-1}^* + F_{i-2}^*)\right] \tag{11}$$

In the previous equations, the subscript i denotes the spatial grid point and the superscript n the time level. The fourth-order accuracy is obtained by alternating the scheme just given with its symmetric variant. To apply this scheme to a two-dimensional problem, the operator-splitting method is used. If L_x and L_y denote the solution operators for the one-dimensional x and y problems, then the solution to Eq. (1) is obtained by

$$Q^{n+2} = L_x L_y L_y L_x Q^n \tag{12}$$

Further details about the method and the advantage of fourth-order schemes can be found in Bayliss et al.[10,11]

The boundary conditions employed on the surface for the Navier-Stokes equations are

$$u = v = 0 \qquad T = T_w \tag{13}$$

over the rigid part of the surface, and

$$u = 0 \qquad v = \frac{\partial w}{\partial t} \qquad T = T_w \tag{14}$$

over the flexible part of the surface.

The pressure boundary conditions are as follows: over the rigid part of the surface the pressure is calculated using the normal momentum equation, and over the flexible part of the surface a linear extrapolation from the interior of the domain is used to find the pressure. We first update the pressure to the new time level by integrating the Navier-Stokes equations and using $\partial w/\partial t$ at the previous time level as a boundary condition; then using the new pressure field, we solve the plate equation to update w.

The inflow conditions are given by

$$Q_{\text{inflow}} = Q_0 + \epsilon_2 \Re[\phi(y)e^{i\omega_2 t}] \tag{15}$$

where Q_0 is the steady-state solution corresponding to a mean flow over a rigid surface, $\Re$ indicates the real part, $\phi(y)$ is the first-mode disturbance eigenvector solution obtained from a compressible stability code, for a given set of boundary-layer parameters (boundary-layer profile and inflow Reynolds number),[12] and ω_2 and ϵ_2 are the frequency and amplitude of the inflow disturbance, respectively. The remaining inflow, outflow, and upper-boundary conditions are the same as in Maestrello et al.[13]

The plate equation is integrated using an implicit finite difference method for structural dynamics developed by Hoff and Pahl.[14] The boundary conditions used to solve the plate equation are those for a clamped plate

$$w = w_x = 0 \qquad \text{at} \qquad x = x_0,\ x_0 + L \tag{16}$$

The problem of transient oscillations is common when trying to solve the time-dependent structural equations. To eliminate the effects of this transient on the flowfield, the plate equation is integrated to obtain a steady-state solution with the acoustic excitation alone. To accelerate the convergence, higher physical damping is used initially; then it is reduced to the desired value progressively. The steady-state displacement, velocity, and acceleration profiles are then used as inputs to the Navier-Stokes calculations, which are then run to eliminate the remaining transient. The time scales of the surface vibration are long compared with the allowable time steps for the Navier-Stokes solver; typically 5×10^{-5} s for the structure and 10^{-7} for Navier-Stokes. Thus there are limits to the length of time for which it is currently feasible to solve the equations of the model. We believe that the data presented here represents an approximation to the steady-state surface response to within the accuracy of the model.

Results and Discussion

Numerical experiments are carried out for a supersonic laminar boundary layer with a freestream Mach number of 2.2, a Reynolds number per meter of 5.25×10^5, and a total temperature of 311 K. The properties of the flexible part of the surface are assumed to be independent of position and are stiffness $D = 1.46$ N · m, mass per unit area $\rho_p h = 2.26$ kg/m^2, and physical damping $\gamma = 131.2$ N · s/m^3. The plate is 0.254 m long and 78.7 μm thick and is clamped between two rigid surfaces. The first seven natural frequencies of the plate are 45, 122, 206, 396, 591, 826, and 1100 Hz. The dimensions of the computational domain are 1.27 m in the downstream distance and 0.0254 m in the vertical distance corresponding to 20 boundary-layer thicknesses. This large value of the vertical distance is chosen to calculate the freestream radiated pressure and has no effect on the numerical results. The number of points used are 301 and 201 in the streamwise and vertical directions, respectively. An exponential stretching is used in the vertical distance to achieve good resolution in the boundary layer.

The different configurations that we compute are shown in Fig. 1: a rigid surface (Fig. 1a), a flexible surface clamped between two rigid ones (Fig. 1b), and an acoustic source placed below the flexible part of the surface (Fig. 1c). The acoustic source emits plane waves at normal incidence to the surface at different frequencies and with a constant sound pressure level. Disturbances are introduced in the flowfield at both the inflow boundary and by acoustic excitation of the surface from below. A two-dimensional TS-type disturbance is introduced at the inflow with a normalized amplitude in u of 0.08 of the freestream and a normalized frequency $F = 2\pi f\nu/U_\infty^2$ of 60×10^{-6} corresponding to a dimensional frequency of $f = 4500$ Hz ($\omega_2 = 2\pi f$). This frequency corresponds to the least stable two-dimensional first mode. In the definition of F, ν is the kinematic viscosity, and U_∞ is the freestream streamwise velocity. Based on linear stability theory, this disturbance is expected to grow and then decay with increasing streamwise distance. To follow the evolution of the disturbance downstream, the mass flux disturbance level in the streamwise direction (ρu) is calculated. First, the streamwise mass flux fluctuation in time is obtained by

$$(\rho u)' = \rho u - \langle \rho u \rangle \tag{17}$$

where $\langle \rho u \rangle$ is the computed mean obtained from integrating the data in time. The integration is performed over one period of the sound source frequency. The disturbance level is then calculated by computing the root mean square (rms) in time of $(\rho u)'$ and then integrating in y,

$$\text{rms} = \langle (\rho u)'^2 \rangle ½ \tag{18}$$

$$G(x) = \int (\text{rms})\, dy \tag{19}$$

Figure 2 shows the results of this calculation for a disturbance propagating over the rigid surface of Fig. 1a and the vibrating surface of Fig. 1c. The various disturbances used are

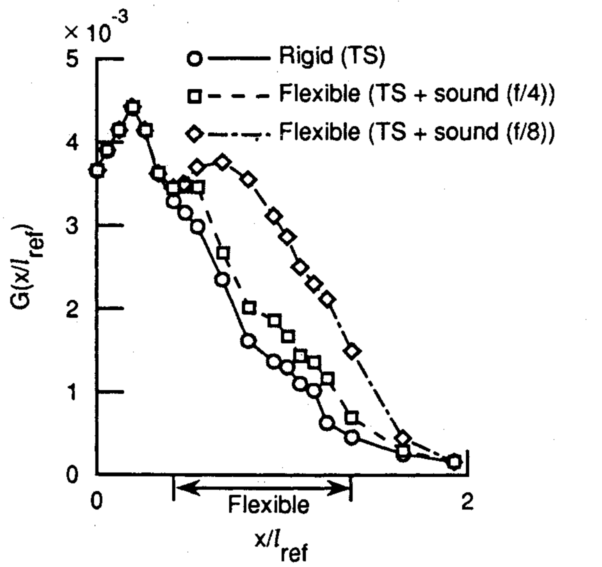

Fig. 2 Comparison of streamwise mass flux disturbance level generated by the interaction of a two-dimensional disturbance with a rigid surface and a vibrating flexible surface at different downstream locations.

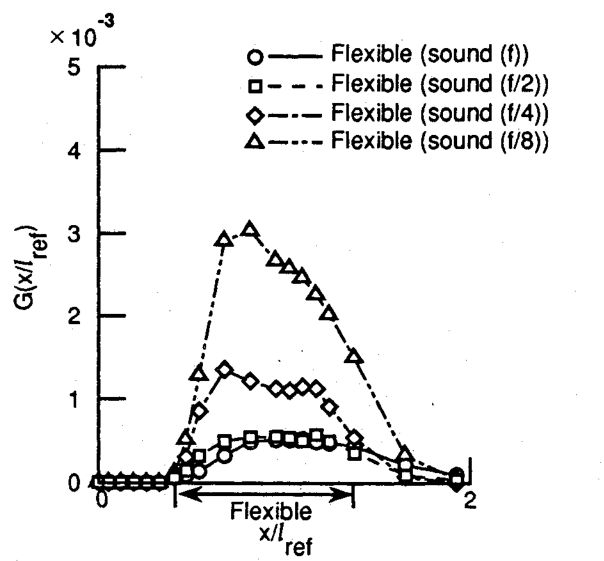

Fig. 3 Effect of sound source frequency on the streamwise mass flux disturbance level at different downstream locations.

indicated in parentheses where f is the TS frequency (4500 Hz). We note that all three computations are graphically indistinguishable upstream of the flexible surface. Over the rigid surface the disturbance grows and then decays as predicted from the linear stability theory. When a sound source emitting plane acoustic waves at a frequency of $f/4$ is used to excite the surface, the interaction between the TS disturbance and the vibrating surface gives rise to a small increase in the disturbance level compared with the rigid surface case. As the frequency of the sound source is reduced to $f/8$, the disturbance level clearly departs from that obtained over a rigid surface. The results indicate that excitation of sufficiently low frequency can be effective in exciting substantial vibrations of the flexible surface. These vibrations can significantly change the resulting evolution of the unsteady disturbances in the flowfield. In the absence of the sound source, the disturbance level over the flexible surface is the same as that over a rigid surface, indicating a weak coupling between the surface and the disturbance.

The effect of sound source frequency was investigated in the absence of the TS-type waves, and the results are shown in Fig. 3. For the same sound pressure level of the acoustic excitation, Fig. 3 shows that the disturbance level introduced by the flexible surface increases as the frequency decreases. For high-frequency excitation, the disturbance level in the boundary layer is nearly uniform over the flexible surface. As the frequency is reduced, the disturbance level grows and is concentrated near the leading edge of the flexible surface. However, in all of the cases the disturbance level decays over the trailing edge and downstream of the flexible surface.

To further explain the differences shown in Fig. 2 between the $f/4$ and $f/8$ frequencies, a comparison of the disturbance level obtained for a rigid surface, a flexible surface excited by sound alone, and a flexible surface excited by a combination of a TS-type wave and sound was made. For a sound source frequency of $f/4$, the disturbance level due to the sound source alone is everywhere less than that of the TS-type disturbance over the rigid surface. Therefore, the level of the combined disturbance over the flexible surface is only slightly higher than that of a rigid surface as is shown in Fig. 4a. However, when the frequency of the sound source is reduced to $f/8$ the level of the disturbance generated by the vibrating surface is higher than that of the TS-type disturbance over the rigid surface. This results in a higher level of the combined disturbances over the flexible surface, Fig. 4b. It is interesting

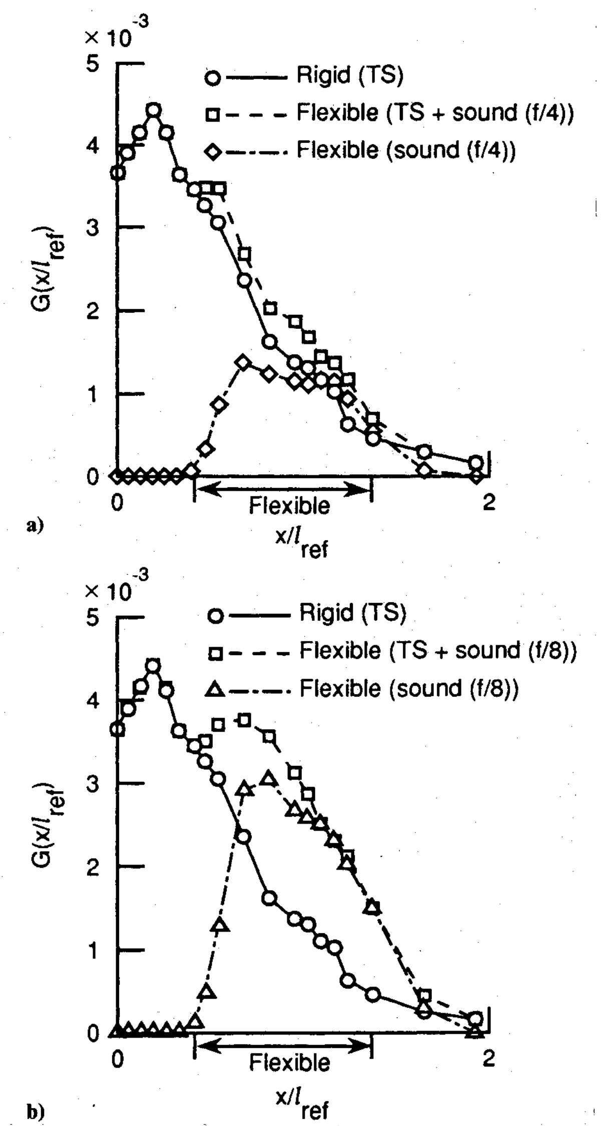

Fig. 4 Comparison of disturbance levels generated by TS-type waves over a rigid surface to that generated by a vibrating flexible surface (no TS waves) and to that generated by the interaction of the TS waves with the vibrating surface: a) sound source frequency of $f/4$, b) sound source frequency of $f/8$.

to note that near the leading edge of the flexible surface the level of the combined disturbances is higher than that of the sound source alone; however, near the trailing edge the two curves coincide. This is an indication that the two disturbances do not simply add up but that there are regions of constructive and destructive interference between the two waves.

Figure 5 shows the instantaneous pressure distribution in the flowfield over the rigid and flexible surfaces. The pressure distribution over the rigid surface is generated by the instability waves, Fig. 5a. However, when the same disturbance propagates over a vibrating flexible surface, it interacts with the pressure disturbance radiated by the surface. Outside the boundary layer, the radiated pressure curves in the direction of the flow and propagates along the Mach line (at a Mach angle of 27 deg). Figure 5b shows the interaction between these two waves when the frequency of the acoustic source is $f/4$. This excitation frequency (1125 Hz) is near the seventh natural frequency of the surface, and therefore its response and near-field radiation patterns are dominated by the seventh

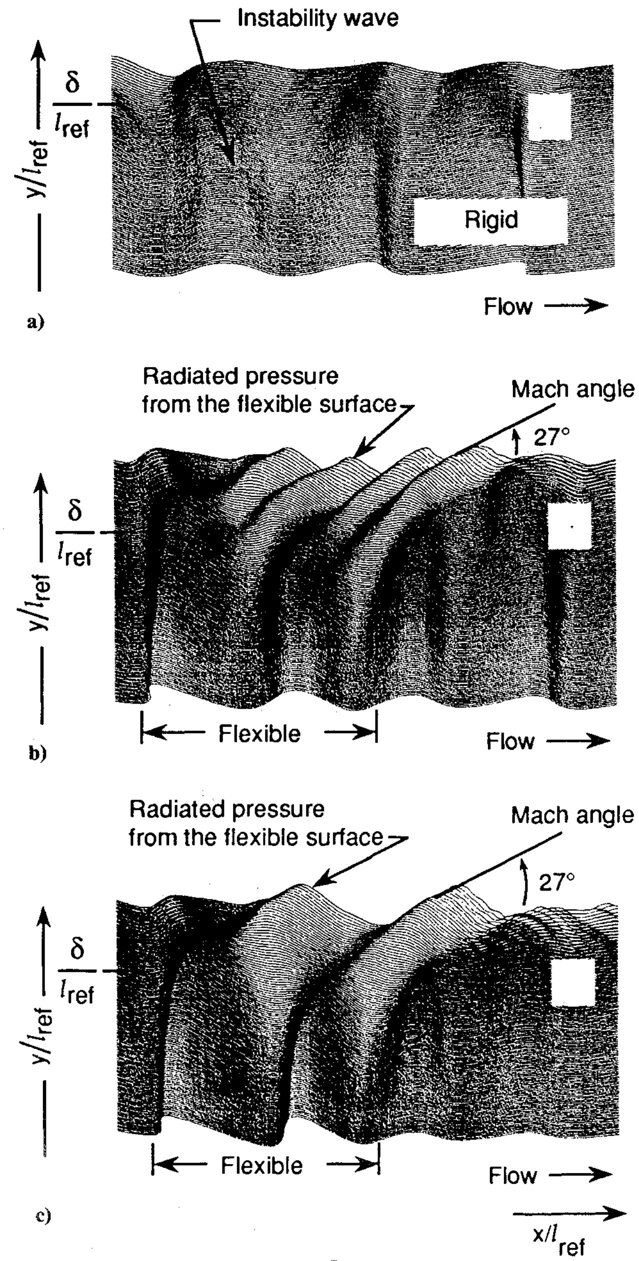

Fig. 5 Instantaneous pressure distribution in the flowfield: a) TS-type waves over a rigid surface, b) TS-type waves over a vibrating flexible surface, sound source frequency $f/4$, c) sound source frequency $f/8$.

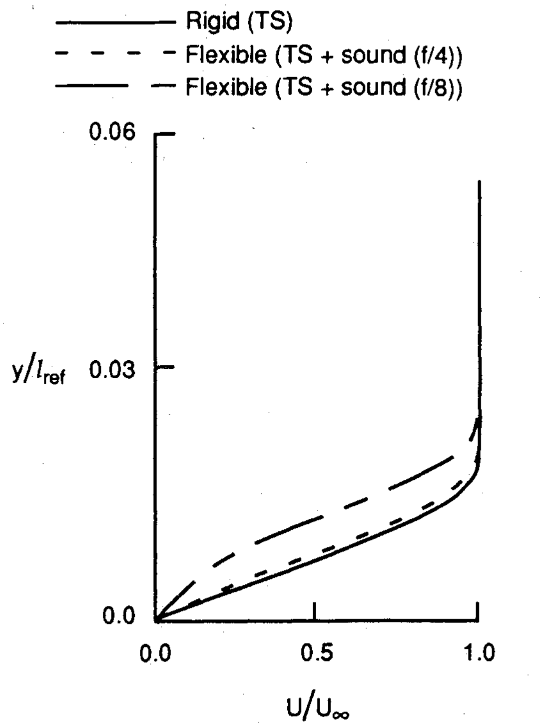

Fig. 6 Comparison of instantaneous velocity profiles at the center of a rigid surface and a vibrating flexible surface.

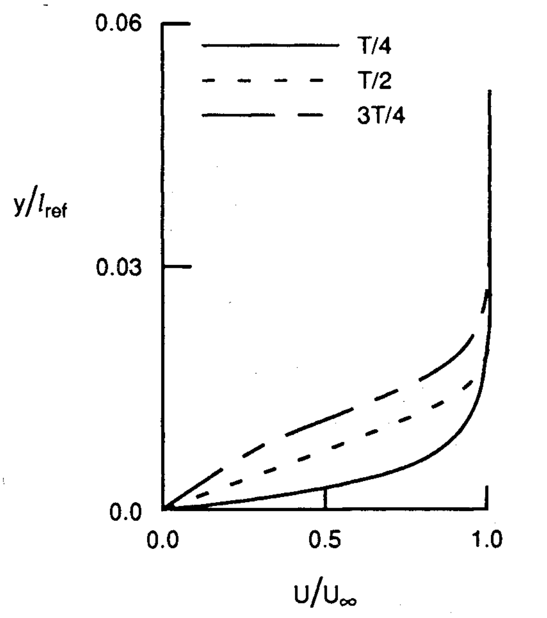

Fig. 7 Time variation of the velocity profile at the center of the vibrating flexible surface, sound source frequency $f/8$ (T is the oscillation period).

mode. These seventh-mode patterns are shown in the pressure distribution of Fig. 5b. Decreasing the sound source frequency to $f/8$ (563 Hz) leads to the excitation of lower modes on the surface. The pressure field shown by Fig. 5c corresponds to that radiated by a third mode. The increase in vibration level and the mode shape of the flexible surface result in greater coupling between flow and structure, which explains the increase in disturbance level for the $f/8$ case. One should note that Figs. 5b and 5c show only a small fraction of a wavelength of the acoustic wave radiated by the surface because of the small vertical dimension (0.0254 m) compared with the acoustic wavelength (0.61 m for $f/8$).

Figure 6 shows a comparison of the instantaneous velocity profiles at the center of the flexible and rigid surfaces for the

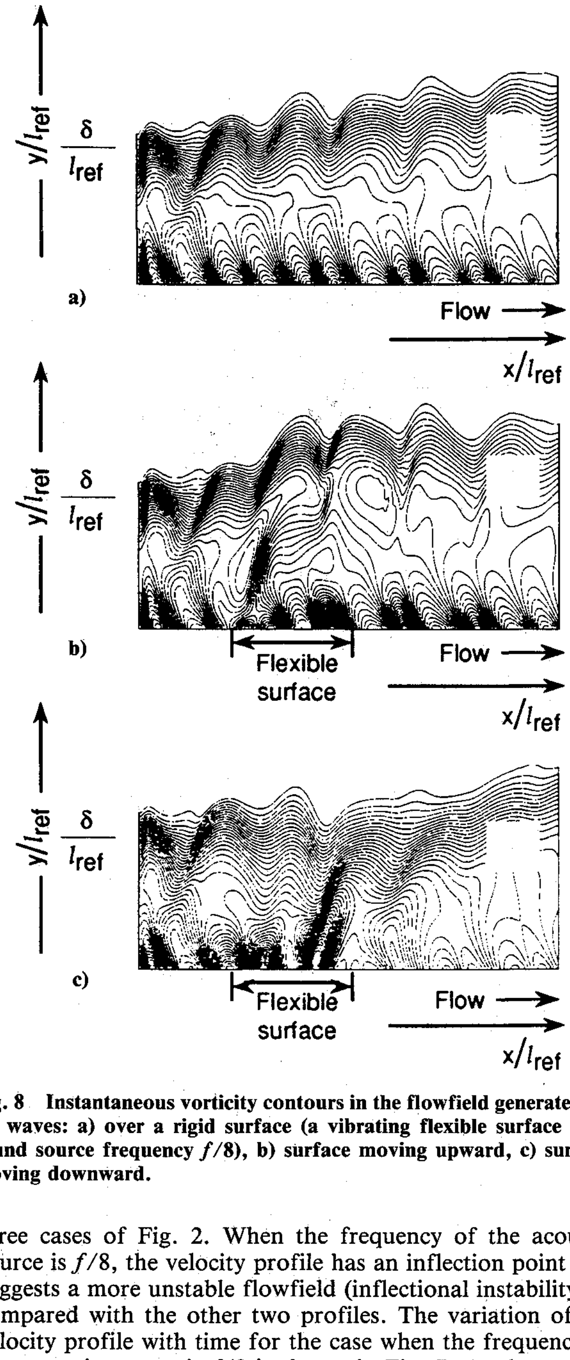

Fig. 8 Instantaneous vorticity contours in the flowfield generated by TS waves: a) over a rigid surface (a vibrating flexible surface with sound source frequency $f/8$), b) surface moving upward, c) surface moving downward.

three cases of Fig. 2. When the frequency of the acoustic source is $f/8$, the velocity profile has an inflection point that suggests a more unstable flowfield (inflectional instability) as compared with the other two profiles. The variation of the velocity profile with time for the case when the frequency of the acoustic source is $f/8$ is shown in Fig. 7. As the surface motion goes through one cycle (based on $f/8$, period T), the velocity profile varies between the upper and lower profiles. The change in the velocity profile leads to a change in boundary-layer thickness. A thicker boundary layer is associated with the upper, less stable profile whereas a thinner boundary layer is obtained for the lower profile. This result indicates that the flexible surface acts like a piston, with blowing and suction phases.

The vorticity contours of the flowfield generated by the TS disturbance over the rigid surface are shown in Fig. 8a, and those generated by the interaction of the TS disturbances with a vibrating flexible surface excited by a sound source of frequency $f/8$ are shown on Figs. 8b and 8c. As the flexible surface moves upward, the vorticity contours cluster near the leading edge of the flexible surface indicating an increase in disturbance level in that region, Fig. 8b, which is in agreement with Figs. 3 and 4. In addition, the vorticity is lifted away from the wall, leading to an increase in boundary-layer thickness. Near the leading edge of the flexible surface, there are indications of possible vortex roll up, which can be a precursor to transition. When the surface is moving downward, the vorticity contours are concentrated near the flexible surface, Fig. 8c. The boundary layer becomes thinner, and there is no indication of vortex roll up.

Conclusions

Based on the results presented here, the following conclusions can be made.

1) The coupling between TS-type waves and a flexible surface is not significant. This result is caused by the fact that the frequencies of the TS-type waves are too high to effectively excite the surface.

2) Acoustic excitation of the flexible surface can effectively excite vibrations of the surface, provided the frequency is sufficiently low (for the given set of structural parameters). In this case, the resulting surface vibration can significantly enhance the level of unsteady disturbances in the flow and change the nature of the flowfield. In particular inflection points can develop in the velocity profile and the incipient formation of vortex rolls can be seen.

3) The effect of the surface vibrations can be transmitted outside of the boundary layer as acoustic radiation.

Acknowledgments

The first author was supported by NASA Langley Research Center under Contract NAS1-19317. Partial support for the third author was also provided under NASA Contracts NAS1-18107 and NAS1-18605 while he was in residence at the Institute for Computer Applications in Science and Engineering (ICASE).

References

[1]Lees, L., and Lin, C. C., "Investigation of the Stability of the Laminar Boundary Layer in a Compressible Fluid," NACA TN 1115, Jan. 1946.

[2]Dunn, D. W., and Lin, C. C., "On the Stability of the Laminar Boundary Layer in a Compressible Fluid," *Journal of Aeronautical Sciences*, Vol. 22, No. 7, 1955, pp. 455–477.

[3]Mack, L. M., "The Stability of the Compressible Laminar Boundary Layer According to a Direct Numerical Solution, Part IV," *Space Programs Summary*, Vol. 37-24, Jet Propulsion Lab., Pasadena, CA, 1963, pp. 271–274.

[4]Mack, L. M., "Stability of the Compressible Laminar Boundary Layer According to a Direct Numerical Solution," AGARD Rept. 97, Pt. I, May 1965, pp. 329–362.

[5]Mack, L. M., "Boundary Layer Linear Stability Theory," AGARD Rept. 709, July 1984, pp. 3-1–3-81.

[6]Mack, L. M., "On the Inviscid Acoustic Mode Instability of Supersonic Shear Flows, Part I: Two-Dimensional Waves," *Theoretical Computational Fluid Dynamics*, Vol. 2, 1990, pp. 97–123.

[7]Frendi, A., Maestrello, L., and Bayliss, A., "Outgoing Acoustic Waves in an Unstable Supersonic Laminar Boundary Layer over a Flexible Surface," *Instability, Transition and Turbulence,* edited by M. Y. Hussaini, A. Kumar, and C. L. Streett, Springer-Verlag, New York, 1992, pp. 337–343.

[8]Miksis, M. J., and Ting, L., "Scattering of an Incident Wave from an Interface Separating two Fluids," *Wave Motion*, Vol. 11, 1989, pp. 545–557.

[9]Gottlieb, D., and Turkel, E., "Dissipative Two-Four Methods for Time Dependent Problems," *Mathematics of Computations*, Vol. 30, 1976.

[10]Bayliss, A., Parikh, P., Maestrello, L., and Turkel, E., "A Fourth Order Scheme for the Unsteady Compressible Navier-Stokes Equations," AIAA Paper 85-1694, July 1985.

[11]Bayliss, A., Maestrello, L., Parikh, P., and Turkel, E., "Numerical Simulation of Boundary Layer Excitation by Surface Heating/Cooling," *AIAA Journal*, Vol. 24, No. 7, 1986, pp. 1095–1101.

[12]El Hady, N. M., "On the Effect of Boundary Layer Growth on the Stability of Boundary Layer Flows," NASA Contractor Rept. 3474, Sept. 1981.

[13]Maestrello, L., Bayliss, A., and Krishnan, R., "On the Interaction Between First and Second Mode Waves in a Supersonic Boundary Layer," *Physics of Fluids A*, Vol. 3, No. 12, 1991, p. 3014–3020.

[14]Hoff, C., and Pahl, P. J., "Development of an Implicit Method with Numerical Dissipation from a Generalized Single-Step Algorithm for Structural Dynamics," *Computer Methods in Applied Mechanical Engineering*, Vol. 67, 1988, pp. 367–385.